

Running Title: Targeted near-infrared fluorescence imaging in breast cancer

1  
2 **Tumor-specific uptake of fluorescent bevacizumab-IRDye800CW microdosing in patients**  
3 **with primary breast cancer: a phase I feasibility study**

4  
5 **Running Title:** Targeted near-infrared fluorescence imaging in breast cancer  
6

7 **Authors:** Laetitia E. Lamberts<sup>1</sup>, Maximillian Koch<sup>2</sup>, Johannes S. de Jong<sup>3</sup>, Arthur L.L. Adams<sup>4</sup>,  
8 Jürgen Glatz<sup>2</sup>, Mariëtte E.G. Kranendonk<sup>3</sup>, Anton G.T. Terwisscha van Scheltinga<sup>1,5</sup>, Liesbeth  
9 Jansen<sup>6</sup>, Jakob de Vries<sup>6</sup>, Marjolijn N. Lub-de Hooge<sup>5</sup>, Carolien P. Schröder<sup>1</sup>, Annelies  
10 Jorritsma- Smit<sup>5</sup>, Matthijs D. Linssen<sup>5</sup>, Esther de Boer<sup>6</sup>, Bert van der Vegt<sup>7</sup>, Wouter B.  
11 Nagengast<sup>8</sup>, Sjoerd G. Elias<sup>9</sup>, Sabrina Oliveira<sup>10</sup>, Arjen J. Witkamp<sup>11</sup>, Willem P.Th.M. Mali<sup>4</sup>,  
12 Elsen Van der Wall<sup>12</sup>, Paul J. van Diest<sup>3</sup>, Elisabeth G.E. de Vries<sup>1</sup>, Vasilis Ntziachristos<sup>2,†</sup>,  
13 Gooitzen M. van Dam<sup>6,13,14,\*;†</sup>

14 **Affiliations:** Department of Medical Oncology<sup>1</sup>, Hospital and Clinical Pharmacy<sup>5</sup>, Department of  
15 Surgery<sup>6</sup>, Department of Pathology<sup>7</sup>, Department of Gastroenterology<sup>8</sup>, Department of Nuclear  
16 Medicine and Molecular Imaging<sup>13</sup>, Department of Intensive Care<sup>14</sup>, University of Groningen,  
17 University Medical Center Groningen, the Netherlands.

18 Department of Pathology<sup>3</sup>, Department of Radiology<sup>4</sup>, Julius Center for Health Sciences and  
19 Primary Care<sup>9</sup>, Division of Cell Biology of the Department of Biology<sup>10</sup>, Department of  
20 Surgery<sup>11</sup>, Department of Medical Oncology<sup>12</sup>, Utrecht University, University Medical Center  
21 Utrecht, the Netherlands.

22 <sup>2</sup>Technische Universität München & Helmholtz Zentrum<sup>3</sup>, München, Germany.

23 † Both authors share last position

24 \*Corresponding author

25

1 **Financial support:**

2 This work was supported by the Center for Translational Molecular Medicine, project  
3 MAMMOTH (grant 03O-201), ERC Advanced grant OnQView and by the Dutch Cancer Society  
4 KWF by a research fellowship to SGE.

5

6 **Conflict of interest:**

7 VN is co-founder of SurgVision BV (Heerenveen, the Netherlands), GMvD and VN are members  
8 of the scientific board of SurgVision BV. GMvD, WBN and PJvD have received an unrestricted  
9 research grant from SurgVision BV for the development en evaluation of image-guided  
10 fluorescence technology and tracers, not related to this study. All consumables (i.e. bevacizumab  
11 and IRDye800CW) were commercially obtained.

12

13 **Corresponding author:**

14 Prof dr Gooitzen M. van Dam, MD, PhD. University Medical Center Groningen, Department of  
15 Surgery, Division of Surgical Oncology BA-11, Hanzeplein 1, 9700 RB Groningen, the  
16 Netherlands. Tel. +31-50-3612283, Fax. +31-50-3614873. E-mail: [g.m.van.dam@umcg.nl](mailto:g.m.van.dam@umcg.nl)

17

18 **Manuscript Information**

19 Word count: 4,698 words

20 Translational relevance statement: 144 words

21 Total number of figures: 5 figures

22 Total number of tables: 1 table

23 Supplemental Material and Methods / Figures: 7 figures, 1 movie and 1 file

24

1 **TRANSLATIONAL RELEVANCE**

2 Tumor-free surgical margins are critical in breast conserving surgery (BCS), as local recurrence  
3 rates increase with positive margins. Molecular imaging is a promising strategy for visualizing  
4 and quantifying tumor-specific molecular characteristics, and potentially improve breast cancer  
5 care in terms of detection, characterization and (non-)surgical treatment strategies. A potential  
6 target for molecular imaging is vascular endothelial growth factor (VEGF)-A, involved in tumor  
7 angiogenesis. Our study shows that systemic administration of the fluorescent bevacizumab-  
8 IRDye800CW tracer is safe in *ex vivo* breast cancer guidance and confirms (tumor-)margin  
9 uptake providing a novel framework for systematic evaluation and validation of fluorescent  
10 tracers in image-guided surgery and drug development. As neo-angiogenesis is a universal tumor  
11 marker, other tumor types like colorectal and esophageal cancer might benefit from fluorescence-  
12 guided molecular endoscopy using bevacizumab-IRDye800CW. This approach is of interest for  
13 surgical guidance, but also for diagnostic purposes, drug development and treatment monitoring.  
14

1 **ABSTRACT**

2 *Purpose:* to provide proof of principle of safety, breast tumor-specific uptake and positive tumor  
3 margin assessment of the systemically administered near-infrared fluorescent (NIRF) tracer  
4 bevacizumab-IRDye800CW targeting vascular endothelial growth factor (VEGF)-A in breast  
5 cancer patients. *Experimental Design:* Twenty patients with primary invasive breast cancer  
6 eligible for primary surgery received 4.5 mg bevacizumab-IRDye800CW as intravenous bolus  
7 injection. Safety aspects were assessed as well as tracer uptake and tumor delineation during  
8 surgery and *ex vivo* in surgical specimens using an optical imaging system. *Ex vivo* multiplexed  
9 histopathology analyses were performed for evaluation of biodistribution of tracer uptake and co-  
10 registration of tumor tissue and healthy tissue. *Results:* None of the patients experienced adverse  
11 events. Tracer levels in primary tumor tissue were higher compared to those in the tumor margin  
12 ( $P < 0.05$ ) and healthy tissue ( $P < 0.0001$ ). VEGF-A tumor levels also correlated with tracer  
13 levels ( $r = 0.63$ ,  $P < 0.0002$ ). All but one tumor showed specific tracer uptake. Two out of 20  
14 surgically excised lumps contained microscopic positive margins detected *ex vivo* by fluorescent  
15 macro- and microscopy and confirmed at the cellular level. *Conclusions:* Our study shows that  
16 systemic administration of the bevacizumab-IRDye800CW tracer is safe for breast cancer  
17 guidance and confirms tumor and tumor-margin uptake as evaluated by a systematic validation  
18 methodology. The findings are a step towards a phase II dose-finding study aimed at *in vivo*  
19 margin assessment and point to a novel drug assessment tool that provides a detailed picture of  
20 drug distribution in tumor tissue.

21

22

23

1 **INTRODUCTION**

2 Breast cancer is the second most common cancer, with 522,000 deaths globally in 2012 and a  
3 rising incidence (1). Surgery is one of the three cornerstones of primary invasive breast cancer  
4 treatment, the other two being radiotherapy and systemic therapy. Tumor-free surgical margins  
5 are critical in breast conserving surgery (BCS), as local recurrence rates increase with positive  
6 resection margins (2-5). Therefore, patients with positive resection margins are often re-operated,  
7 causing higher surgical risks, poorer cosmetic results, psychological and physical burden and  
8 higher healthcare costs. Currently, pre-operative imaging and tactile information are used during  
9 breast surgery to determine the size, localization and extent of the area that has to be removed.  
10 However, the efficacy of this approach is poor, with positive margin rates of 20% to 40% being  
11 reported worldwide (6).

12 Molecular imaging is a promising strategy to improve this efficacy; it can be used to  
13 visualize and quantify tumor-specific molecular characteristics, and could potentially improve  
14 breast cancer care in terms of detection, characterization and surgical and non-surgical  
15 management strategies. A potential target for molecular imaging in breast cancer is vascular  
16 endothelial growth factor (VEGF)-A, a soluble dimeric glycoprotein that is involved in tumor  
17 angiogenesis (7,8). VEGF-A is frequently overexpressed in breast cancers with an expression rate  
18 of ~73% compared to normal breast tissue (9). It can therefore serve as a more generic tracer  
19 target (10-11) without pre-selection of patients compared to other potential targets such as human  
20 epidermal growth factor receptor 2 (HER2), which is overexpressed in only 10 to 20% of primary  
21 breast cancers (12-14).

1           The registered humanized monoclonal antibody bevacizumab not only neutralizes all  
2 VEGF-A isoforms, but can also be used as a radiolabeled imaging agent in combination with  
3 single photon emission computed tomography (SPECT) and positron emission tomography  
4 (PET) (15). Successful and specific imaging has been performed in patients with melanoma, renal  
5 cell cancer, neuroendocrine tumors and breast cancer using <sup>111</sup>In- and <sup>89</sup>Zr-radiolabeled  
6 bevacizumab (11,15-19). In these studies, a systemic total microdose of 4.5 mg labeled  
7 bevacizumab, i.e.  $\leq 30$  nmol adhering to the definition of microdosing for proteins according to  
8 FDA/EMA guidelines (20) and as described separately for proteins by Kummar et al (21), was  
9 used which is sub-therapeutic compared to the therapeutic dose of 5-15 mg/kg bodyweight (22-  
10 24). In a recent PET imaging study with <sup>89</sup>Zr-bevacizumab in 23 primary breast cancer patients,  
11 25 of 26 tumors (96%) were visualized by PET 4 days after <sup>89</sup>Zr-bevacizumab tracer injection  
12 with tumor-to-normal tissue ratios of 1.4-10.3 (19). These results prompted us to design an  
13 optical imaging study based on the microdosing concept of using a therapeutic antibody as  
14 targeting moiety in patients undergoing breast cancer surgery.

15           Recently, optical fluorescence imaging has become suitable for clinical translation due to  
16 its favorable characteristics such as absence of ionizing radiation, inherently low-cost technology,  
17 and its possibilities for real-time, intra- and post-operative imaging. Two phase I feasibility  
18 studies in respectively patients with colorectal cancer imaged with a chimeric fluorescein  
19 conjugated Carcino Embryonic Antigen (CEA) targeted antibody (25) and ovarian cancer patients  
20 using folate-fluorescein isothiocyanate (FITC, light emission at 400-650 nm) targeting the folate  
21 receptor-alpha, demonstrated the great potential of optical imaging during surgery using a clinical  
22 prototype camera (26). However, clinical implementation studies have been obstructed by  
23 characteristics such as the limited penetration depth of fluorescent dyes such as fluorescein with

1 emission in the visible light spectrum, the negative effects of optical properties such as  
2 absorption, scattering and the autofluorescence of tissue in the visible spectrum. To reduce  
3 background fluorescence and autofluorescence and increase tissue penetration, near infrared  
4 fluorescent (NIRF) dyes must be used that have excitation wavelengths between 700-900 nm  
5 (27). More recently, Burggraaf et al demonstrated c-met targeted endoscopy fluorescence  
6 imaging in humans using a fluorescent dye of 650 nm (28), whereas Rosenthal et al have  
7 demonstrated the feasibility of using the therapeutic monoclonal antibody cetuximab targeting  
8 Epidermal Growth Factor Receptor (EGFR), as the targeting moiety of a NIRF tracer in patients  
9 with head- and neck cancer (29). Additionally, the clinical application of a protease-activatable  
10 tracer has been reported in patients with soft tissue sarcoma and breast cancer (30).

11       Using bevacizumab conjugated to the NIRF dye IRDye800CW (peak absorption 778 nm,  
12 peak emission 795 nm), we decided to determine if this approach could be used for intraoperative  
13 guidance in breast cancer surgery, combined with a novel systematic analytic methodology for ex  
14 vivo evaluation of tumor-specificity and microdistribution. Bevacizumab-IRDye800CW showed  
15 high levels of accumulation in human breast cancer bearing mouse tumors (31), leading to Good  
16 Manufacturing Practice (GMP) production of clinical grade bevacizumab-IRDye800CW for  
17 human use (32). In conjunction with the progress in the development of NIR intra-operative  
18 optical imaging systems for clinical applications, we initiated this first in-human clinical study of  
19 clinical grade bevacizumab-IRDye800CW in breast cancer patients.

20       The primary aims of our feasibility study were to provide proof of principle of safety,  
21 tumor-specific uptake and tumor margin assessment of the intravenously administered NIRF  
22 microdose tracer bevacizumab-IRDye800CW, targeting VEGF-A in patients with primary  
23 invasive breast cancer, as validated *ex vivo* by multiplex advanced pathology imaging.

1 **MATERIALS AND METHODS**

2

3 **Trial Design**

4 The study was a two center, first in human, two-stage, non-randomized, non-blinded, prospective,  
5 feasibility study in patients with histologically proven breast cancer scheduled for surgery  
6 (registered at [www.clinicaltrials.gov](http://www.clinicaltrials.gov), identifier NCT01508572). Primary endpoints were the  
7 occurrence of serious adverse events (SAE, adverse events were classified according to the  
8 National Cancer Institute Common Terminology Criteria for Adverse Events (Version 4.0)) and  
9 accumulation of bevacizumab-IRDye800CW in breast cancer tissue and surrounding tissue in  
10 surgical specimen by fluorescence macroscopy and microscopy. Additional information is  
11 provided in Supplementary Materials and Methods, section “*Trial Design*”. The Institutional  
12 Review Board (IRB) of the University Medical Center Groningen (UMCG) approved the study,  
13 with local agreement of the University Medical Center Utrecht (UMCU). All patients gave  
14 written informed consent.

15 **Bevacizumab-IRDye800CW Preparation and Injection**

16 Clinical grade bevacizumab-IRDye800CW was produced in the GMP facility of the UMCG by  
17 labeling bevacizumab (Roche AG) and IRDye800CW-NHS (LI-COR Biosciences Inc.) under  
18 regulated conditions as described previously (31). The molecular weight of the protein  
19 bevacizumab is 149 kDa. The fluorescent dye has a molecular weight of 1,166 kDa. With an  
20 average conjugation ratio of 1:4 protein:IRDye800CW, the total molecular weight is 153,7 kDa.  
21 This means for our 4.5 mg tracer dose bevacizumab-IRDye800CW 26 nmol of bevacizumab-  
22 IRDye800CW, adhering to the FDA/EMA regulations of microdosing for proteins and according  
23 to the Task Force on Methodology for the Development of Innovative Cancer Therapies

1 (MDICT) (20,21). Additional information is provided in the Supplementary Material and  
2 Methods, section “*Bevacizumab-IRDye800CW Preparation and Injection*”.

### 3 **Surgical Procedures and Specimen Handling**

4 Patients underwent mastectomy or lumpectomy with or without a sentinel lymph node (SLN)  
5 procedure or axillary LN dissection, according to standard-of-care procedures and guidelines  
6 applicable for breast cancer in The Netherlands (33). During the study period, the positive margin  
7 rate for the University Medical Center Groningen was 7.8% and for the University Medical  
8 Center it was 5.2%.

9 In short, the SLN procedure was carried out by peri-tumoral injection of Technetium-99m nano-  
10 colloid followed by lymph scintigraphy after 2-3 hours. During surgery a hand-held gamma  
11 counter was used to detect the radioactive signal from the SLN. After the first patient, the  
12 protocol was amended to omit patent blue V (Guerbet Asia Pacific) for visualization of the SLN  
13 if possible, as this dye interfered with the fluorescent signal after systemic microdosing 4.5 mg  
14 bevacizumab-IRDye800CW in this patient during surgery.

15 During surgery, images were recorded at several pre-defined time points during removal  
16 of the tumor and SLN with the optical imaging system (for further details see Supplementary  
17 Material, section “*Optical Imaging System*”). A baseline image was recorded before incision of  
18 the breast, followed by imaging of the tumor, before removal of the tumor (lumpectomy or  
19 mastectomy) at a distance suitable for the fluorescent signal (on average 10-15 cm above the  
20 operating field), but not interfering with the sterile field of surgery. Using the optical imaging  
21 system prior to incision at the maximum field-of-view (FOV), the presence of a fluorescence  
22 signal was determined either in the tumor or axillary region. Identified (S)LNs were imaged prior  
23 to excision. After removal of the tumor and SLN, the surgical field was inspected again for  
24 remaining fluorescent signals. The surgical approach could only be adapted to the intraoperative

1 findings if this would not have a negative impact on the actual outcome of the surgical procedure  
2 as judged by the attending breast cancer surgeon (authors LJ, JdV and AJW) in terms of cosmetic  
3 outcome and impaired wound healing. Subsequently, excised tumor tissue and SLN(s) were  
4 imaged *ex vivo* off-table directly after removal. Next, the surgical specimen was processed by the  
5 pathologist for *ex vivo* analysis of tumor samples according to standard procedures and including  
6 imaging of the specimen as described in the subsection ‘Ex vivo analyses of tumor samples’. For  
7 all tumors besides determination of size, extent, presence of *in situ* carcinoma, expression of  
8 estrogen receptor (ER), progesterone receptor (PR) and HER2 histological grading and typing  
9 according to the modified Bloom and Richardson and WHO guidelines was also performed  
10 according to standard clinical practice.

#### 11 **Follow up**

12 Adverse events occurring through approximately 2 weeks after surgery were recorded as  
13 spontaneously reported by patients or at an outpatient visit.

#### 14 **Ex vivo analyses of tumor samples**

15 The following subsections are provided in the Supplementary Material and Methods, section “*Ex*  
16 *vivo analyses of tumor samples*”: i) Imaging fresh surgical specimen, ii) Imaging FFPE blocks  
17 and slides, iii) Bevacizumab-IRDye800CW (34) and VEGF-A quantification, iv)  
18 Immunohistochemistry, v) Fluorescence microscopy, vi) Multiplex Advanced Pathology Imaging  
19 (MAPI) methodology.

#### 20 **Statistical Analysis**

21 Details on statistical analysis and power calculations for detecting potentially clinically relevant  
22 bevacizumab-IRDye800CW breast accumulation in patient with primary breast cancer is  
23 provided in Supplemental Material, section “*Statistical Analysis*”.

24

1 **RESULTS**

2 **Patient Characteristics**

3 Between March 2012 and August 2014, we enrolled 20 patients with breast cancer (including one  
4 male patient) in the study. Patient and tumor characteristics are summarized in Table 1. Most  
5 patients had an invasive ductal carcinoma (n=17, 85%), and three had an invasive ductulobular  
6 carcinoma. Tumor size determined by pathology ranged from 6 mm to 38 mm (median 20 mm)  
7 in diameter. Histological analyses after surgery of the tumor showed Bloom-Richardson-Elston  
8 histology grade 1 in 6 tumors, grade 2 in 10 tumors and grade 3 in 4 tumors. Estrogen receptor  
9 (ER) status was positive in 18 patients (90%), progesterone receptor (PR) status was positive in  
10 14 patients (70%), and HER2 expression scores were negative in 13 patients (65%), 1+ in five  
11 patients, 2+ in one patient and 3+ in one patient. In three patients, all the excised tissue was  
12 required for standard histological examination due to the small tumor sizes of 6 mm. Two  
13 patients (10%) undergoing BCS through a lumpectomy had a positive resection margin on  
14 standard histopathological examination, 18 none.

15 No adverse events related to the tracer injection occurred in any of the patients, nor aberrations in  
16 hematology or blood chemistry levels. In none of the patients tumor recurrence occurred during  
17 follow-up after surgery.

18 **Intra-operative Imaging**

19 Specimens from two patients were identified with a microscopic irradical resection (i.e. the  
20 positive margin) upon histopathological analysis (Fig. 1 and Supplemental. Fig. S1). In both  
21 patients a fluorescent signal was detectable at the positive resection margin of the excised lump  
22 (Fig. 1A-C), although not visible during surgery, but clearly visible on the back table during the  
23 surgical procedure and after bread-loaf slicing (Fig. 1D-F). The paraffin block (Fig. 1G - 1I) also  
24 showed a clear positive signal at the tumor site. Hematoxylin and eosin stain (H/E, Fig. 1J)

1 findings were corroborated by fluorescence flatbed scanning (Fig. 1K) and overlay image (Fig.  
2 1L). This confirmed the presence of bevacizumab-IRDye800CW in the tumor area and the  
3 designated positive margin in both patients. Supplemental Fig. S1 shows the surgical specimen  
4 from the second patient with a positive margin, visualized with our standard operating procedure  
5 for *ex vivo* processing. Fluorescence imaging shows strong signals at the vicinity of the margin in  
6 the bread-loaf slices (Fig. S1, panel A), which was confirmed by NIR optical imaging of paraffin  
7 blocks (Fig. S1, panel B, tumor is demarcated by red segmentation), H/E staining (Fig. S1, panel  
8 C), and fluorescence flatbed scanning (Fig. S1, panel D and E). With one exception, we detected  
9 a fluorescent signal in the excised specimens of all patients who were injected with bevacizumab-  
10 IRDye800CW. In the first patient, a male with breast cancer, in whom we could not detect a  
11 fluorescent signal *ex vivo*, a fluorescent signal prior to incision in the breast was visible but  
12 disappeared upon injection of patent blue (Patent Blue V Sodium Guerbet 2.5% solution for  
13 injection, 1 mL peritumoral injection) as part of the sentinel lymph node (SLN) procedure. For  
14 the remaining 19 patients, patent blue was omitted within the SLN protocol and accordingly  
15 approved by the local IRB. It was concluded that the disappearance of the NIR fluorescence  
16 originating from the systemic injection of a microdose of bevacizumab-IRDye800CW in the  
17 tissue specimen was due to complete absorbance by the abundant peritumoral injection of patent  
18 blue and therefore subsequently omitted. Excised specimens were imaged by flatbed scanning of  
19 the paraffin blocks. Patients who were not injected with bevacizumab-IRDye800CW (negative  
20 controls) did not show fluorescent signals above background levels in tumor areas (Supplemental  
21 Fig. S2). In one patient, the skin was very fluorescent and in one patient a fibroadenoma adjacent  
22 to the tumor showed a clear fluorescent signal. In all patients a Standard Operating Procedure for  
23 *Ex Vivo* Processing of Surgical Specimen was applied (Fig. 2).

24

## 1 **Bevacizumab-IRDye800CW Blood and Tissue Concentrations**

2           The whole blood concentrations of bevacizumab-IRDye800CW decreased during 14 days  
3 after injection (Fig. 3A). The bevacizumab-IRDye800CW concentration in tumor tissue was  
4 higher compared to the margin ( $P < 0.05$ ) or surrounding non-cancerous tissue ( $P < 0.0001$ ) (Fig.  
5 3B). VEGF-A levels differed between tumor and surrounding tissue ( $P < 0.001$ ) and between  
6 margin and surrounding tissue, ( $P < 0.05$ ) but not between tumor and margin (not significant)  
7 (Fig. 3C). Bevacizumab-IRDye800CW and VEGF-A concentrations by ELISA correlated in the  
8 tumor area ( $r = 0.63$ ,  $P = 0.0002$ ) (panel D), but not significantly at the margin or surrounding  
9 non-cancerous tissue (Fig. 3D-F). Additional SDS-PAGE analysis of tumor lysates of three  
10 patients, confirmed the intactness of the bevacizumab-IRDye800CW tracer within the tumor.

## 11 **Fluorescence Imaging and Tumor Margins**

12           To compare macroscopic fluorescence imaging with tumor margins, two methods were  
13 used: tumor area assessment by defining four tumor margin zones distant from the tumor and by  
14 segmentation (Fig. 4). After flatbed scanning (Fig. 4, panel A) and H/E staining of the paraffin  
15 block (Fig. 4, panel D), four margin zones of 5 x 20 mm were defined (tumor area, 0.5 cm, 1.0  
16 cm, 1.5 cm) and scanned (Fig. 4, panel B), after which the mean fluorescence intensity (MFI) was  
17 determined (Fig. 4C). The MFI of the tumor area differed from the other three tumor margin  
18 zones (tumor vs. 0.5 cm, tumor vs. 1.0 cm, tumor vs. 1.5 cm, all  $P < 0.0001$ ).

19           Similarly, segmentation for separating tumor, stroma and fat was performed on the  
20 excised specimen after H/E staining (Fig. 4E, F and G). Next, the segmented areas were  
21 superimposed on the fluorescence flatbed scans (Fig. 4E), and the MFI was calculated (Fig. 4H).  
22 Tumor segmented areas had a higher MFI compared to stroma ( $P < 0.0001$ ) and fat ( $P < 0.0001$ ),  
23 which also translated into a significant difference in target-to-background ratios for tumor/stroma  
24 versus tumor/fat ( $P < 0.001$ ) (Supplemental Fig. S2). In two patients with a positive margin, the

1 margin was fluorescent, while in the remaining 18 patients with a negative margin there was also  
2 no fluorescence in the resection margin. In 90% of all patients there was adjacent / complete  
3 overlap of bevacizumab-IRDye800CW and VEGF-A immunohistochemistry staining and in 10%  
4 no overlap (Fig. 5).

5

### 6 **Multiplex Advanced Pathology Imaging (MAPI)**

7 For a more detailed analysis of the distribution of bevacizumab-IRDye800CW in tumor tissue, a  
8 standardized operating procedure (SOP) for macro- and microscopic mapping was performed at a  
9 macroscopic level as depicted in Fig. 2 and at the cellular level in Supplemental Fig. S3 – S5.

10 H/E staining of 4 µm tissue slides (Fig. S3, panel A and B) was compared to fluorescence  
11 scanning (Fig. S3, panel C and D). In a superimposed image, both modalities were compared on a  
12 macroscopic and microscopic level (Fig. S3, panel E and F). Fluorescence signal was clearly  
13 identified in a tumor sprout surrounded by blood vessels and collagen-rich stroma (rectangle, Fig.  
14 S3, panel B, D and F). NIR fluorescence microscopy compared to co-localization of H/E staining  
15 for tumor (margin) specificity clearly indicated tumor-specific staining of bevacizumab-  
16 IRDye800CW (Fig. S3, panel G and H).

17 For qualitative co-localization of bevacizumab-IRDye800CW with other biomarkers such  
18 as VEGF-A expression, CD34 staining for microvessel density and presence of collagen, MAPI  
19 was used (Supplemental Movie S1). Fluorescent bevacizumab-IRDye800CW scans were  
20 pseudocolored green, whereas hematoxylin-DAB/VEGF-A staining color intensities were color  
21 deconvoluted into pseudocolor red and superimposed with the pseudocolor green bevacizumab-  
22 IRDye800CW scans.

23 Supplemental Fig. S4 shows the co-localization of bevacizumab-IRDye800CW, H/E,  
24 VEGF-A, collagen and CD34 in breast cancer and a satellite lesion. A clear co-localization of

1 fluorescence intensities as determined by fluorescence imaging (Fig. S4, panel A-D) is present  
2 within the tumor area (dotted lines). This was confirmed with H/E staining (Fig. S4, panel E),  
3 segmentation (Fig. S4, panel F), pseudocolor green bevacizumab-IRDye800CW flatbed scan  
4 (Fig. S4, panel G) and superimposed H/E with pseudocolor green (Fig. S4, panel H).  
5 Furthermore, co-localization of fluorescence and VEGF-A staining (Fig. S4, panel I), collagen  
6 (Fig. S4, panel M) and CD34 (Fig. S4, panel Q) could be visualized as such. Additional data is  
7 provided for co-localization in ductal carcinoma in situ (DCIS) in Supplemental Fig. S5.

8 In 18/20 patients, lymph nodes were excised. Only three patients had a tumor positive sentinel  
9 lymph node, 13 patients had a negative sentinel lymph node. Two additional patients had lymph  
10 nodes with macrometastases: one of them had clinical suspicious macrometastatic lymph nodes,  
11 confirmed by ultrasound guided biopsy and axillary lymph node dissection. Only in this patient  
12 we could even clearly identify fluorescence activity intraoperatively within the lymph node  
13 dissection specimen in situ, confirmed by ex vivo fluorescence and histopathological analysis  
14 (Supplemental Fig. S6). There was no difference in VEGF-A IHC staining between tumor-  
15 positive lymph nodes and negative lymph nodes (n=104 lymph node tissue blocks). Co-  
16 localization of NIR fluorescence showed mainly fluorescence surrounding the tumor cells within  
17 a lymph node (Supplemental Fig. S6), whereas in a tumor-negative lymph node it was mainly  
18 centrally located in the lymph node (Supplemental Fig. S7).

19

20

21

22

23

1  
2

## DISCUSSION

3           In this first in-human study using a NIRF antibody-based tracer in a microdose regimen,  
4 administration of bevacizumab-IRDye800CW was safe with sufficient tumor-specific tracer  
5 uptake for margin assessment in primary breast cancer tissue. A novel framework of systematic  
6 *ex vivo* macroscopic imaging and fluorescent image analyses of excised specimen, fresh tissue  
7 slices, paraffin blocks and tissue slides showed tumor-specific tracer uptake, thus clearly  
8 distinguishing the tumor margins within normal healthy breast tissue. This framework provides a  
9 novel tool for evaluation and validation of fluorescent tracers in image-guided surgery. NIR light  
10 has low tissue absorption characteristics, mainly caused by hemoglobin, and low  
11 autofluorescence properties compared to fluorescent dyes in the visible light (27). In BCS, a  
12 negative microscopic resection margin is of great value in order to reduce a re-operation or the  
13 risk of recurrent disease (35), even after adjuvant radiotherapy. A NIRF tumor-specific tracer is  
14 therefore the most suitable in terms of sensitivity and specificity whether (microscopic) residual  
15 tissue is present and should accordingly be excised.

16           Most prior optical imaging efforts in breast cancer patients used the non-targeted NIRF  
17 tracer ICG, which binds to plasma proteins. This has been tested extensively for lymphatic  
18 mapping in breast cancer (36-40). In breast cancer patients, ICG had SLN identification rates  
19 comparable to standard-of-care radiotracers and blue dyes (40). However, ICG is unsuitable due  
20 to the limiting formulation and quenching characteristics of the dye for simple and  
21 straightforward conjugation to targeting moieties, like antibodies, nanobodies or small peptides.  
22 This precludes its use for tumor-specific targeting by NIRF imaging, as in the present study. At  
23 this point, two clinical landmark studies have been published on the use of fluorescent targeted  
24 antibodies. One study targeting Carcino Embryonic Antigen (CEA) in colorectal cancer (25), and

1 more recently Epidermal Growth Factor Receptor (EGFR) in head- and neck cancer (29). Several  
2 approaches have been used showcasing the potential of fluorescence imaging in humans, varying  
3 from single-dose to dose-escalation designs differing from our micro-dosing approach. In  
4 particular, the *ex vivo* validation steps for visualization of tumor microdistribution of the NIR  
5 fluorescent tracer and its relationship to histological immunohistochemical parameters provides a  
6 framework which was not reported earlier in previous clinical studies in for example fluorescein-  
7 conjugated CEA-targeted imaging in colorectal cancer (25), folate receptor- $\alpha$  imaging in ovarian  
8 cancer (26), the study of Rosenthal et al using cetuximab-IRDye800CW in head- and neck cancer  
9 (29) and a protease activatable probe in soft tissue sarcoma and breast cancer (30). Therefore, the  
10 impact of our study is that it provides the necessary framework of evaluation and reporting of  
11 future clinical studies of fluorescence image-guided surgery. The *in vivo* targeting characteristics  
12 of a GMP fluorescent tracer by applying as a first step the microdosing concept, and thus a low  
13 risk of potential adverse events, delivers data on the targeting characteristics of the tracer and  
14 subsequently the format for *ex vivo* analyses. If such a study provides the data for tumor specific  
15 targeting, then a subsequent dose-finding or diagnostic accuracy study can be carried out with a  
16 higher degree of definitive data. As mentioned by Kummar et al (21), ‘microdosing studies are  
17 designed with the objective to establish at the very earliest opportunity – before a large numbers  
18 of patients have been accrued and exposed to potential drug-associated toxicity – whether an  
19 agent is targeting its biological marker in a tumor, and consequently whether further clinical  
20 development is warranted’ and thus allows selection of tracer candidates more likely to be  
21 developed successfully, but also helps in determination of the dosing-scheme for the subsequent  
22 Phase II-III clinical studies.

23 Although *ex vivo* imaging confirmed tumor specific uptake in our study, the absolute  
24 fluorescent signal intensities of the targeted tracer were too low to identify tumor margins *in situ*

1 during actual surgery, for which several explanations are possible. First, the tracer dose used in  
2 this study may have been too low to reach the threshold for detecting tumor-specific signal intra-  
3 operatively originating from microscopic irradiated tumor margins. Nevertheless, 90% of all  
4 patients using microdosing bevacizumab-IRDye800CW showed adjacent or complete overlap  
5 with VEGF-A expression measured by IHC. Second, due to the fact that usually surgical  
6 incisions in BCS are small, this might imply that insufficient excitation light reaches the surgical  
7 cavity or wound bed or vice versa that emitted NIR light originating from the tracer cannot be  
8 collected by the optical imaging system. This might be solved by applying a sterile NIR  
9 laparoscope or endoscope close within the wound bed. Third, even with a higher dose,  
10 improvements in the sensitivity of the camera system, such as correction algorithms and state-of-  
11 the-art charge-coupled device (CCD) chips, may be required for intra-operative detection of  
12 bevacizumab-IRDye800CW.

13 By increasing the tracer dose to still sub-therapeutic doses, a signal above the threshold of  
14 healthy surrounding autofluorescent signal can be expected, and intra-operative detection of the  
15 fluorescent signal in tumor tissue may be feasible. This has recently been shown by Rosenthal et  
16 al. up to a maximum dose of  $62.5 \text{ mg/m}^2$  of intravenously injected cetuximab-IRDye800CW in  
17 patients with head and neck cancer (HNSCC) up (29). Similarly, a large clinically proven safe  
18 dose range is still available for a bevacizumab NIR tracer. For example, patients treated for  
19 colorectal cancer with neo-adjuvant bevacizumab being dosed at 10-15 mg/kg every 3 weeks  
20 undergo surgery around 6 weeks after the last bevacizumab dose to avoid wound healing  
21 problems. With a half-life of 20 days, the remaining circulating bevacizumab level is around 160  
22 mg at that time. This would translate into a minimum 180 mg flat bevacizumab dose, to be  
23 injected 3 days before surgery, without increased risk of impaired wound healing. In future  
24 studies, we therefore suggest a dose escalation starting around 10 mg and increasing up to the

1 potential maximum of 180 mg. The total costs for microdosing and the procedural costs are  
2 estimated to be \$1800. As VEGF-A is overexpressed in >70% of all patients with breast cancer  
3 eligible for breast conserving surgery, pre-selection by applying a <sup>89</sup>Zr-bevacizumab PET  
4 imaging study seems redundant and imposes in ~30% of the patients an increased radiation risk  
5 which does not outweigh the risks associated with an injection of a non-radioactive fluorescent  
6 tracer.

7         In our clinical study we used the NIR optical imaging system not only during surgery, but  
8 also post-operatively during pathological examination to image the complete excised specimen,  
9 after bread-loaf slicing, in paraffin blocks and on tissue slides. These slice images showed a clear  
10 fluorescent signal at the site of the tumor in fresh tissue, as confirmed by fluorescence scanning  
11 and microscopy. Fluorescence-guided pathology may thereby assist the pathologist in assessing  
12 the important tissue parts or for sensitive sampling, such as tumor margin assessment of a  
13 mastectomy or lumpectomy specimens. Moreover, during surgery, the pathologist can  
14 immediately report to the surgeon whether all tumor has been excised or if margins show a  
15 fluorescent signal, which might indicate the presence of tumor.

16 By using multiplex advanced pathology imaging (MAPI), a systemically injected bevacizumab-  
17 IRDye800CW fluorescent tracer was cross-correlated with the presence of tumor (using H/E),  
18 VEGF-A expression (by IHC and ELISA), collagen and microvessel density. Next to  
19 visualization of other targets with antibodies, smaller fragments like nanobodies targeting  
20 specific tumor markers such as carbonic anhydrase IX, HER2, and carcinoembryonic antigen  
21 have been developed more recently for imaging solid tumors. This could also be validated by  
22 NIR optical imaging (in situ and ex vivo) and MAPI in future translational clinical studies (41-  
23 43). Moreover, the present study has shown that MAPI can be used *ex vivo* to cross-correlate the

1 fluorescent-labeled therapeutic drug bevacizumab and its tumor-specific targeting and local  
2 tumor distribution in humans by using excised specimens. This can be done with both  
3 macroscopic and microscopic imaging. This novel co-localization methodology provides a  
4 reproducible platform in drug development and subsequent dose-finding studies at the tissue and  
5 cellular level for other antibodies (therapeutic or otherwise), nanobodies and small peptides as  
6 targeting moiety.

7         As neo-angiogenesis is a universal tumor marker, other tumor types may also benefit from  
8 fluorescence imaging using bevacizumab-IRDye800CW. For example, HNSCC, colorectal and  
9 esophageal cancer may be suitable for such imaging, as these tumors are located more  
10 superficially, leading to higher fluorescence signals and less negative impact on surrounding  
11 tissue (i.e. scattering, penetration issues). Currently, three studies are ongoing to determine  
12 feasibility of a fluorescent endoscope attached to the camera system after administration of 4.5  
13 mg bevacizumab-IRDye800CW intravenously to detect rectal cancer, esophageal cancer and pre-  
14 malignant and malignant polyps in familial adenomatous polyposis (ClinicalTrials.gov identifiers  
15 NCT01972373, NCT02129933 and NCT02113202). This approach is therefore of interest not  
16 only for tumor visualization and characterization in intra-operative surgical guidance, but also for  
17 diagnostic purposes, drug development and treatment monitoring (42).

18         In conclusion, this is the first clinical study to demonstrate safety and feasibility of the  
19 NIR fluorescent tracer bevacizumab-IRDye800CW for tumor-specific optical imaging in patients  
20 with primary breast cancer. Probably, because the administered dose (i.e. microdose of 4.5 mg –  
21 26 nmol) was low, in situ intra-operative tumor margin detection was not possible. However,  
22 immediate NIR optical imaging of the excised specimen in patients with a positive margin  
23 confirmed reliable margin assessment by fluorescence. Therefore, *ex vivo* imaging was highly  
24 feasible and correlated well with VEGF-A quantification and microscopic analyses of the tumor

1 site of targeting. Microscopic analyses did not show a complete overlay of the fluorescent signal  
2 and the VEGF-A staining. This is probably because bevacizumab-IRDye800CW targets the  
3 soluble and extracellular matrix-bound splice variant 121 of VEGF-A (10,11), whereas the  
4 applied IHC staining mainly detects intracellular VEGF-A expression. For intra-operative *in situ*  
5 imaging purposes, fluorescent intensity values could be optimized using higher tracer doses that  
6 are still well below the therapeutic dosing scheme of bevacizumab, such as recently described for  
7 cetuximab-IRDye800CW.

8 We have therefore initiated a subsequent phase II dose-finding study to determine the  
9 optimal dose for intra-operative use in patients with primary breast cancer  
10 ([www.clinicaltrials.gov](http://www.clinicaltrials.gov): NCT02583568).

11

1    **REFERENCES**

- 2    1. International Agency for Research on Cancer. World cancer statistics. GLOBOCAN 2012.
- 3    2. Waljee JF, Hu ES, Newman LA, Alderman AK. Predictors of re-excision among women  
4    undergoing breast-conserving surgery for cancer. *Ann Surg Oncol* 2008;15:1297-1303.
- 5    3. Biglia N, Maggiorotto F, Liberale V, Bounous VW, Sqro LG, Pecchio S, et al. Clinical-  
6    pathologic features, long term-outcome and surgical treatment in a large series of patients with  
7    invasive lobular carcinoma (ILC) and invasive ductal carcinoma (IDC). *Eur J Surg Oncol*  
8    2013;39:455-60.
- 9    4. Park CC, Mitsumori M, Nixon A, Recht A, Connolly J, Gelman R, et al. Outcome at 8 years  
10   after breast-conserving surgery and radiation therapy for invasive breast cancer: Influence of  
11   margin status and systemic therapy on local recurrence. *J Clin Oncol* 2000;18:1668-75.
- 12   5. Chagpar AB, Martin RC, Hagendoorn LJ, Chao C, McMasters KM. Lumpectomy margins  
13   are affected by tumor size and histologic subtype but not by biopsy technique. *Am J Surg*  
14   2004;188:399-402.
- 15   6. Pleijhuis RG, Graafland M, de Vries J, Bart J, de Jong JS, van Dam GM. Obtaining adequate  
16   surgical margins in breast-conserving therapy for patients with early-stage breast cancer: current  
17   modalities and future directions. *Ann Surg Oncol* 2009;16:2717-30.
- 18   7. Ferrara N, Davis-Smyth T. The biology of vascular endothelial growth factor. *Endocr Rev*  
19   1997;18:4-25.

- 1 8. Amini A, Masoumi Moghaddam S, Morris DL, Pourgholami MH. The critical role of vascular  
2 endothelial growth factor in tumor angiogenesis. *Curr Cancer Drug Targets* 2012;12:23-43.
- 3 9. Liu Y, Tamimi RM, Collins LC, Schnitt SJ, Gilmore HL, Connolly JL, et al. The association  
4 between vascular endothelial growth factor expression in invasive breast cancer and survival  
5 varies with intrinsic subtypes and use of adjuvant systemic therapy: Results from the Nurses'  
6 Health Study. *Breast Cancer Res Treat* 2011;129:175-84.
- 7 10. Viacava P, Naccarato AG, Bocci G, Fanelli G, Aretini G, Lonobile A, et al. Angiogenesis and  
8 VEGF expression in pre-invasive lesions of the human breast. *J Pathol* 2004;204:140-46.
- 9 11. Nagengast WB, Hooge MN, van Straten EM, Kruijff S, Brouwers AH, den Dunnen WF, et  
10 al. VEGF-SPECT with <sup>111</sup>In-bevacizumab in stage III/IV melanoma patients. *Eur J Cancer*  
11 2011;47:1595-1602.
- 12 12. Slamon DJ, Godolphin W, Jones LA, Holt JA, Wong SG, Keith DE, et al. Studies of the  
13 HER-2/neu proto-oncogene in human breast and ovarian cancer. *Science* 1989;244:707-12.
- 14 13. Slamon D, Eiermann W, Robert N, Pienkowski T, Martin M, Press M, et al. Breast Cancer  
15 international Research Group, Adjuvant trastuzumab in HER2-positive breast cancer. *New Engl J*  
16 *Med* 2011;365:1273-83.
- 17 14. Lamberts LE, Williams SP, Terwisscha van Scheltinga AG, Lub-de Hooge MN, Schröder  
18 CP, Gietema JA, et al. Antibody positron emission tomography imaging in anticancer drug  
19 development. *J Clin Oncol* 2015;33:1491-1504.

- 1 15. Desar IM, Stillebroer AB, Oosterwijk E, Leenders WP, van Herpen CM, van der Graaf WT,  
2 et al. <sup>111</sup>In-bevacizumab imaging of renal cell cancer and evaluation of neoadjuvant treatment  
3 with the vascular endothelial growth factor receptor inhibitor sorafenib. J Nucl Med  
4 2010;51:1707-15.
- 5 16. Scheer MG, Stollman TH, Boerman OC, Verrijp K, Sweep FC, Leenders WP, et al. Imaging  
6 liver metastases of colorectal cancer patients with radiolabelled bevacizumab: Lack of correlation  
7 with VEGF-A expression. Eur J Cancer 2008;44:1835-40.
- 8 17. Oosting SF, Brouwers AH, van Es SC, Nagengast WB, Oude Munnink TH, Lub-de Hooge  
9 MN, et al. <sup>89</sup>Zr-bevacizumab PET visualizes heterogeneous tracer accumulation in tumor lesions  
10 of renal cell carcinoma patients and differential effects of antiangiogenic treatment. J Nucl Med  
11 2015;56:63-69.
- 12 18. van Asselt SJ, Oosting SF, Brouwers AH, Bongaerts AH, de Jong JR, Lub-de Hooge MN, et  
13 al. Everolimus reduces <sup>89</sup>Zr-bevacizumab tumor uptake in patients with neuroendocrine tumors. J  
14 Nucl Med 2014;55:1087-92.
- 15 19. Gaykema SB, Brouwers AH, Lub-de Hooge MN, Pleijhuis RG, Timmer-Bosscha H, Pot L, et  
16 al. <sup>89</sup>Zr-bevacizumab PET imaging in primary breast cancer. J Nucl Med 2013;54:1014-18.
- 17 20. FDA Guidance for Industry, Investigators and Reviewers / Exploratory IND studies, January  
18 2006, FDA Center for Drug Evaluation and Research:  
19 <http://www.fda.gov/downloads/drugs/guidancecomplianceregulatoryinformation/guidances/ucm0>  
20 [78933.pdf](http://www.fda.gov/downloads/drugs/guidancecomplianceregulatoryinformation/guidances/ucm078933.pdf).

- 1 21. Kummar S, Doroshow JH, Tomaszewski JE, Calvert AH, Lobbezoo M, Giaccone G, et al.  
2 Task Force on Methodology for the Development of Innovative Cancer Therapies (MDICT).  
3 Phase 0 clinical trials: recommendations from the Task Force on Methodology for the  
4 Development of Innovative Cancer Therapies. *Eur J Cancer* 2009;45:741-6.
- 5 22. Vokes EE, Salgia R, Karrison TG. Evidence-based role of bevacizumab in non-small cell  
6 lung cancer. *Ann Oncol* 2013;24:6-9.
- 7 23. Hurwitz HI, Tebbutt NC, Kabbinavar F, Giantonio BJ, Guan ZZ, Mitchell L, et al. Efficacy  
8 and safety of bevacizumab in metastatic colorectal cancer: Pooled analysis from seven  
9 randomized controlled trials. *Oncologist* 2013;18:1004-12.
- 10 24. Escudier B, Bellmunt J, Négrier S, Bajetta E, Melichar B, Bracarda S, et al. Phase III trial of  
11 bevacizumab plus interferon alfa-2a in patients with metastatic renal cell carcinoma (AVOREN):  
12 Final analysis of overall survival. *J Clin Oncol* 2010;28:2144-50.
- 13 25. Folli S, Wagnières G, Pèlerin A, Calmes JM, Braichotte D, Buchegger F, et al.  
14 Immunophotodiagnosis of colon carcinomas in patients injected with fluoresceinated chimeric  
15 antibodies against carcinoembryonic antigen. *Proc Natl Acad Sci U S A* 1992;89:7973-7.
- 16 26. van Dam GM, Themelis G, Crane LMA, Harlaar NJ, Pleijhuis RG, Kelder W, et al.  
17 Intraoperative tumor-specific fluorescence imaging in ovarian cancer by folate receptor- $\alpha$   
18 targeting: First in-human results. *Nat Med* 2011;17:1315-19.
- 19 27. Frangioni JV. New technologies for human cancer imaging. *J Clin Oncol* 2008;26:4012-21.
- 20 28. Burggraaf J, Kamerling IM, Gordon PB, Schrier L, de Kam ML, Kales AJ, et al. Detection of

- 1 colorectal polyps in humans using an intravenously administered fluorescent peptide targeted  
2 against c-Met. Nat Med. 2015 Aug;21(8):955-61.
- 3 29. Rosenthal EL, Warram JM, de Boer E, Chung TK, Korb ML, Brandwein-Gensler M, et al.  
4 Safety and tumor-specificity of cetuximab-IRDye800 for surgical navigation in head and neck  
5 cancer. Clin Cancer Res 2015;21:3658-66.
- 6 30. Whitley MJ, Cardona DM, Lazarides AL, Spasojevic I, Ferrer JM, Cahill J, et al. A mouse-  
7 human phase Ico-clinical trial of a protease-activated fluorescent probe for imaging cancer. Sci  
8 Transl Med 2016;8:320ra4.
- 9 31. Terwisscha van Scheltinga AG, van Dam GM, Nagengast WB, Ntziachristos V, Hollema H,  
10 Herek JL, et al. Intraoperative near-infrared fluorescence tumor imaging with vascular  
11 endothelial growth factor and human epidermal growth factor receptor 2 targeting antibodies. J  
12 Nucl Med 2011;52:1778-85.
- 13 32. Ter Weele EJ, Terwisscha van Scheltinga AG, Linssen MD, Nagengast WB, Lindner I,  
14 Jorritsma-Smit A, de Vries EG, Kosterink JG, Lub-de Hooge MN. Development, preclinical  
15 safety, formulation, and stability of clinical grade bevacizumab-800CW, a new near infrared  
16 fluorescent imaging agent for first in human use. Eur J Pharm Biopharm 2016;104:226-34.
- 17 33. Dutch Guidelines for Breast Cancer 2.0, Richtlijnen Database 2012-2016, IKNL:  
18 [http://richtlijnendatabase.nl/en/richtlijn/breast\\_cancer/breast\\_cancer.html](http://richtlijnendatabase.nl/en/richtlijn/breast_cancer/breast_cancer.html).
- 19 34. Oliveira S, Cohen R, Walsum MS, van Dongen GA, Elias SG, van Diest PJ, et al. A novel  
20 method to quantify IRDye800CW fluorescent antibody probes ex vivo in tissue distribution  
21 studies. Eur J Nucl Med Mol Imaging Res 2012;25:50.

- 1 35. Pleijhuis RG, Kwast AB, Jansen L, Vries J, Lanting R, Bart J, Wiggers T, van Dam Gm,  
2 Siesling S. A validated web-based nomogram for predicting positive surgical margins following  
3 breast-conserving surgery as a predictive tool for clinical decision-making. *Breast* 2013;22:773-9.
- 4 36. Troyan SL, Kianzad V, Gibbs-Strauss SL, Gioux S, Matsui A, Oketokoun R, et al. The  
5 FLARE intraoperative near-infrared fluorescence imaging system: A first-in-human clinical trial  
6 in breast cancer sentinel lymph node mapping. *Ann Surg Oncol* 2009;16:2943-52.
- 7 37. Murawa D, Hirche C, Dresel S, Hünnerbein M. Sentinel lymph node biopsy in breast cancer  
8 guided by indocyanine green fluorescence. *Br J Surg* 2009;96:1289-94.
- 9 38. Hojo T, Nagao T, Kikuyama M, Akashi S, Kinoshita K. Evaluation of sentinel node biopsy  
10 by combined fluorescent and dye method and lymph flow for breast cancer. *Breast* 2010;19:210-  
11 13.
- 12 39. Schaafsma BE, Mieog JS, Hutteman M, van der Vorst JR, Kuppen PJ, Löwik CW, et al. The  
13 clinical use of indocyanine green as a near-infrared fluorescent contrast agent for image-guided  
14 oncologic surgery. *J Surg Oncol* 2011;104:323-32.
- 15 40. Mieog JS, Troyan SL, Hutteman M, Donohoe KJ, van der Vorst JR, Stockdale A, et al.  
16 Toward optimization of imaging system and lymphatic tracer for near-infrared fluorescent  
17 sentinel lymph node mapping in breast cancer. *Ann Surg Oncol* 2011;18:2483-91.
- 18 41. Luker GD, Luker KE. Optical imaging: Current applications and future directions. *J Nucl*  
19 *Med* 2008;49:1-4.

- 1 42. de Boer E, Harlaar NJ, Taruttis A, Nagengast WB, Rosenthal EL, Ntziachristos V, et al.
- 2 Optical innovations in surgery. *Br J Surg* 2015;102:e56-72.
  
- 3 43. Rosenthal EL, Warram JM, Basilion JP, Biel MA, Bogyo M, Bouvet M, et al. Successful
- 4 translation of fluorescence navigation during oncologic surgery: a consensus report. *J Nucl Med*
- 5 2015;57:144-50.
  
- 6

1 **Table 1.**

| Characteristic                            | N  | %    | Median<br>(range) |
|---|----|------|-------------------|
| Gender, female                            | 19 | 95   |                   |
| Surgery                                   |    |      |                   |
| Lumpectomy                                | 11 | 55   |                   |
| Mastectomy                                | 9  | 45   |                   |
| Side tumor                                |    |      |                   |
| Right                                     | 8  | 40   |                   |
| Left                                      | 12 | 60   |                   |
| Age (y)                                   |    |      | 65 (46 – 81)      |
| Tumor size (mm)                           |    |      |                   |
| Conventional imaging before surgery       |    |      |                   |
| Ultrasound                                |    |      | 15 (4 - 40)       |
| MRI (n=1)                                 |    |      | 28                |
| Pathology                                 |    |      | 20 (6 - 38)       |
| <b>HISTOLOGY</b>                          |    |      |                   |
| <b>DUCTAL CARCINOMA</b>                   | 17 | 85   |                   |
| <b>DUCTULOLOBULAR</b>                     | 3  | 15   |                   |
| <b>CARCINOMA</b>                          |    |      |                   |
| Bloom-Richardson-Elston grade             |    |      |                   |
| Grade 1                                   | 6  | 30   |                   |
| Grade 2                                   | 10 | 50   |                   |
| Grade 3                                   | 4  | 20   |                   |
| Receptor status                           |    |      |                   |
| ER (positive)                             | 18 | 90   |                   |
| PR (positive)                             | 14 | 70   |                   |
| HER2 (IHC 3+ or 2+ with FISH positive)    | 1  | 5    |                   |
| Ductal carcinoma in situ component (n=15) | 2  | 13.3 |                   |
| Grade 1                                   | 10 | 66.7 |                   |
| Grade 2                                   | 2  | 13.3 |                   |
| Grade 3                                   | 1  | 6.7  |                   |
| Intracystic papillary carcinoma           |    |      |                   |
| Pathological tumor stage                  |    |      |                   |
| T1a                                       | 0  | 0    |                   |
| T1b                                       | 4  | 20   |                   |
| T1c                                       | 6  | 30   |                   |
| T2  | 10 | 50   |                   |
| Pathological nodal stage                  |    |      |                   |
| N0  | 13 | 65   |                   |
| N1  | 7  | 35   |                   |
| Positive surgical margin                  | 2  | 10   |                   |

1  
2  
3  
4  
5  
6  
7  
8  
9  
10  
11  
12  
13  
14  
15  
16  
17  
18  
19  
20  
21  
22  
23

**Legends of Tables and Figures**

**Table 1. Patient demographic and pathological characteristics.** Tumor grade according to the Bloom–Richardson–Elston system (grade 1, 2, or 3).

**Figure 1. Optical Imaging of Positive Tumor Margin.** In one of the two patients (see also Supplemental Fig. S1) with a positive margin (tumor characteristics: lobular carcinoma, diameter 2.3 cm, Bloom-Richardson-Elston grade 1, mitotic activity index (MAI) 2, estrogen receptor positive, progesterone receptor negative, HER2 negative), the bevacizumab-IRDye800CW tracer in the positive margin (black and white arrows) could be detected *ex vivo* by optical imaging of the excised lump (panel A white-light, panel B fluorescence, panel C overlay with pseudocolor). Bread-loaf slicing (panel D-F) and the paraffin block (panel G-I) is shown for the corresponding fluorescent signal. Hematoxylin/eosin (H/E) stain (panel J), fluorescence flatbed scanning (panel K) and image overlay of panel J and K (panel L) is shown for the 4 μm slide (\* = skin with suture in place, \*\* = satellite tumor foci, red/white/black dashed line = tumor outline, white/black arrow = positive tumor margin).

1  
2 **Figure 2. Standard Operating Procedure for *Ex Vivo* Processing of Surgical Specimen.** Upon  
3 excision during surgery, the entire fresh specimen was cut into bread-loaf slices and imaged by  
4 the optical imaging system in overlay images of white light and fluorescence mode (panel A,  
5 fluorescence = green pseudocolor, asterisk = tumor). Next, tissue was embedded into paraffin  
6 blocks and overlay images of white light and fluorescence were taken (panel B, red = tumor  
7 border, green = pseudocolor for fluorescence). In panel C, hematoxylin/eosin (H/E) staining is  
8 shown of slides from the same paraffin blocks (red = tumor localization) for co-localization  
9 purposes with the fluorescence images. Prior to H/E staining, the paraffin blocks were scanned on  
10 a flatbed scanner (panel D, depicted in mean fluorescence intensity (MFI)), and also depicted as a  
11 Manhattan intensity graph in panel E.

12  
13 **Figure 3. *Ex Vivo* Quantification of Bevacizumab-IRDye800CW and VEGF-A in Whole**  
14 **Blood and Tissue.** Blood concentration levels (mean  $\pm$  standard deviation) of bevacizumab-  
15 IRDye800CW (ng/ml) decreased 14 days after injection of the tracer (panel A). In tumor tissue  
16 biopsies there was a higher concentration of bevacizumab-IRDye800CW (ng/mL/mg of weight  
17 biopsy tissue) compared to the tumor margin (\* =  $P < 0.05$ ) and surrounding (non-cancerous)  
18 tissue (\*\*\*\* =  $P < 0.0001$ ) (panel B). VEGF-A (pg/mg) concentrations differed significantly  
19 between tumor vs. surrounding tissue (\*\*\*) =  $P < 0.001$ ) and margin vs. surrounding tissue (\* =  $P$   
20  $< 0.05$ ), but not between tumor area and margin (ns) (panel C). Bevacizumab-IRDye800CW and  
21 VEGF-A correlated in the tumor area ( $r = 0.63$ ,  $P = 0.0002$ ) (panel D), which was not apparent at  
22 the margin (panel E), or in surrounding non-cancerous tissue (panel F).

23  
24

1  
2 **Figure 4. Macroscopic Fluorescence Tumor Margin Assessment.** Paraffin blocks were inked  
3 for margin assessment as standard of care and subsequently imaged by macroscopic fluorescence  
4 imaging, followed by H/E staining (panel A). By defining four tumor margin zones distant from  
5 the tumor (i.e. tumor area, 0.5 cm, 1.0 cm and 1.5 cm, panel B), the mean fluorescence intensity  
6 (MFI) was calculated (panel C). MFI of the tumor site was higher than in the tumor margin zones  
7 (\*\*\*) ( $P < 0.0001$ ). **Macroscopic Segmentation of Fluorescence Tissue Localization.** Paraffin  
8 blocks were scanned (panel A), stained for hematoxylin/eosin (H/E) (panel D), and subsequently  
9 segmented (panel E and F). For each tissue type the region-of-interest (ROI) was delineated  
10 (panel G, tumor [RED], stroma [GREEN] and fat [BLUE]). Per ROI, mean fluorescence intensity  
11 (MFI) was calculated and compared (panel F). Tumor tissue had a higher MFI compared to  
12 stroma and fat (\*\*\*) ( $P < 0.001$ ).

13  
14 **Figure 5. Co-localization of Vascular Endothelial Growth Factor-A (VEGF-A) and**  
15 **Bevacizumab-IRDye800CW.** Color deconvolution (DAB color layers were converted to red-  
16 black images) of immunohistochemistry staining for VEGF expression is depicted in red. Near-  
17 infrared fluorescence of bevacizumab-IRDye800CW is depicted in green. Between VEGF-A and  
18 bevacizumab-IRDye800CW localization there was in 90% of the patients adjacent / complete  
19 overlap (18/20 patients) and no overlap in 10% of the patients (2/20 patients).

Figure 1

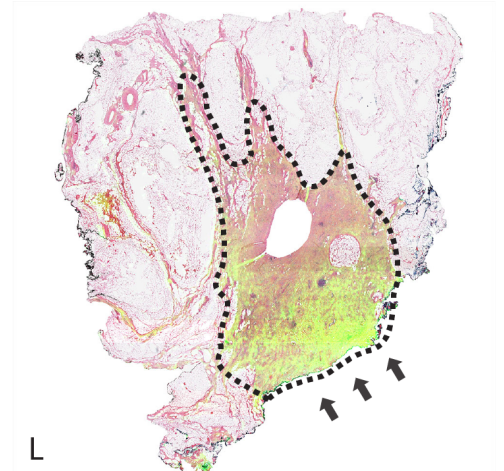
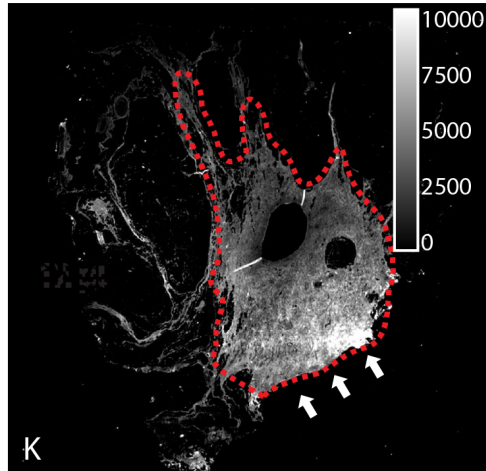
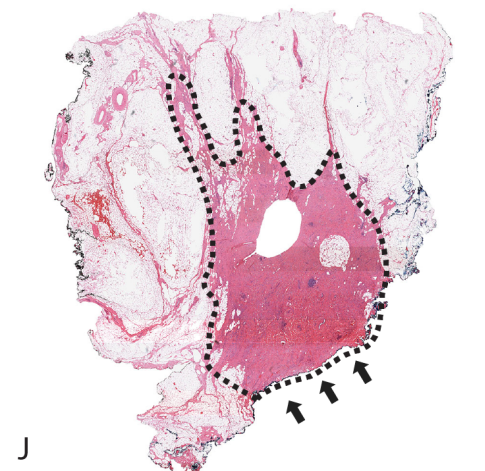
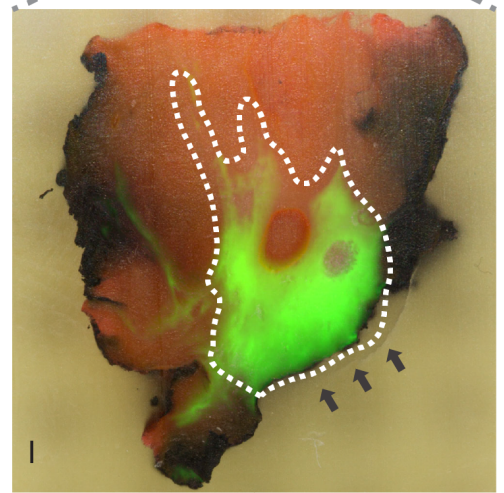
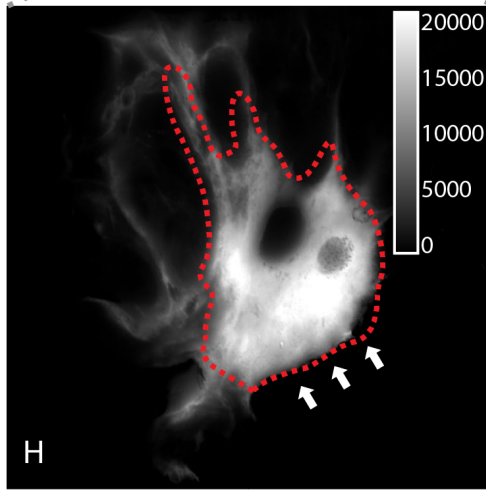
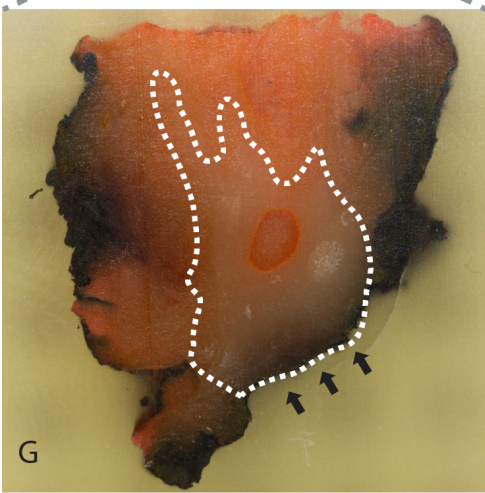
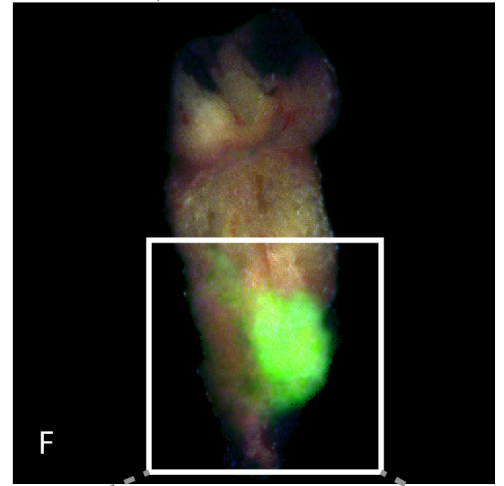
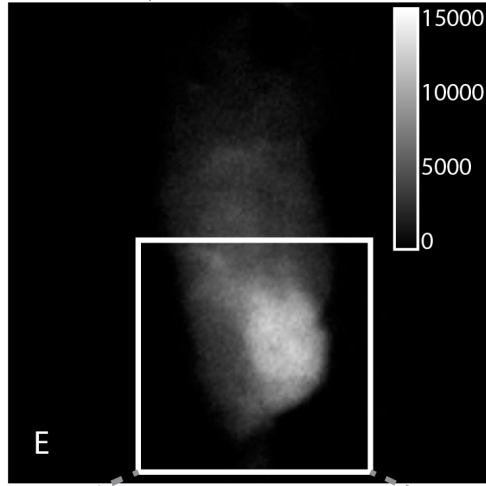
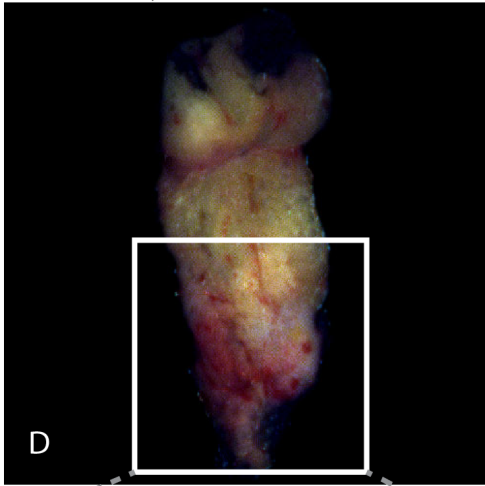
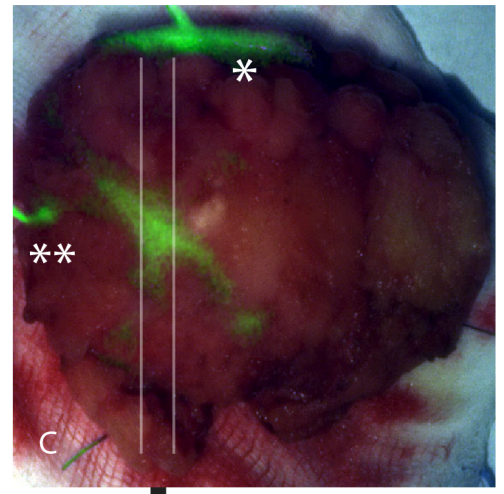
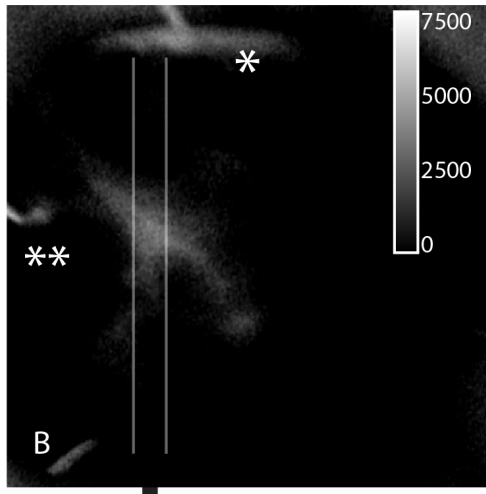
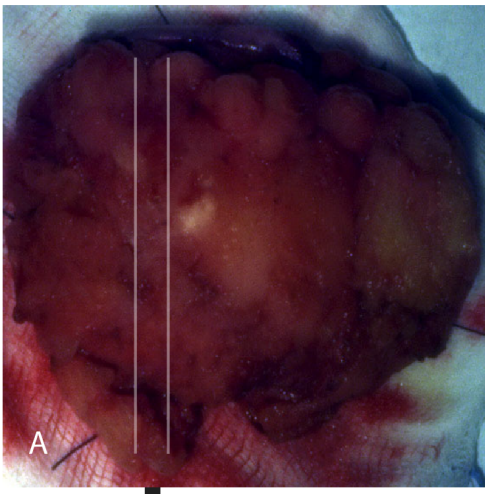


Figure 2

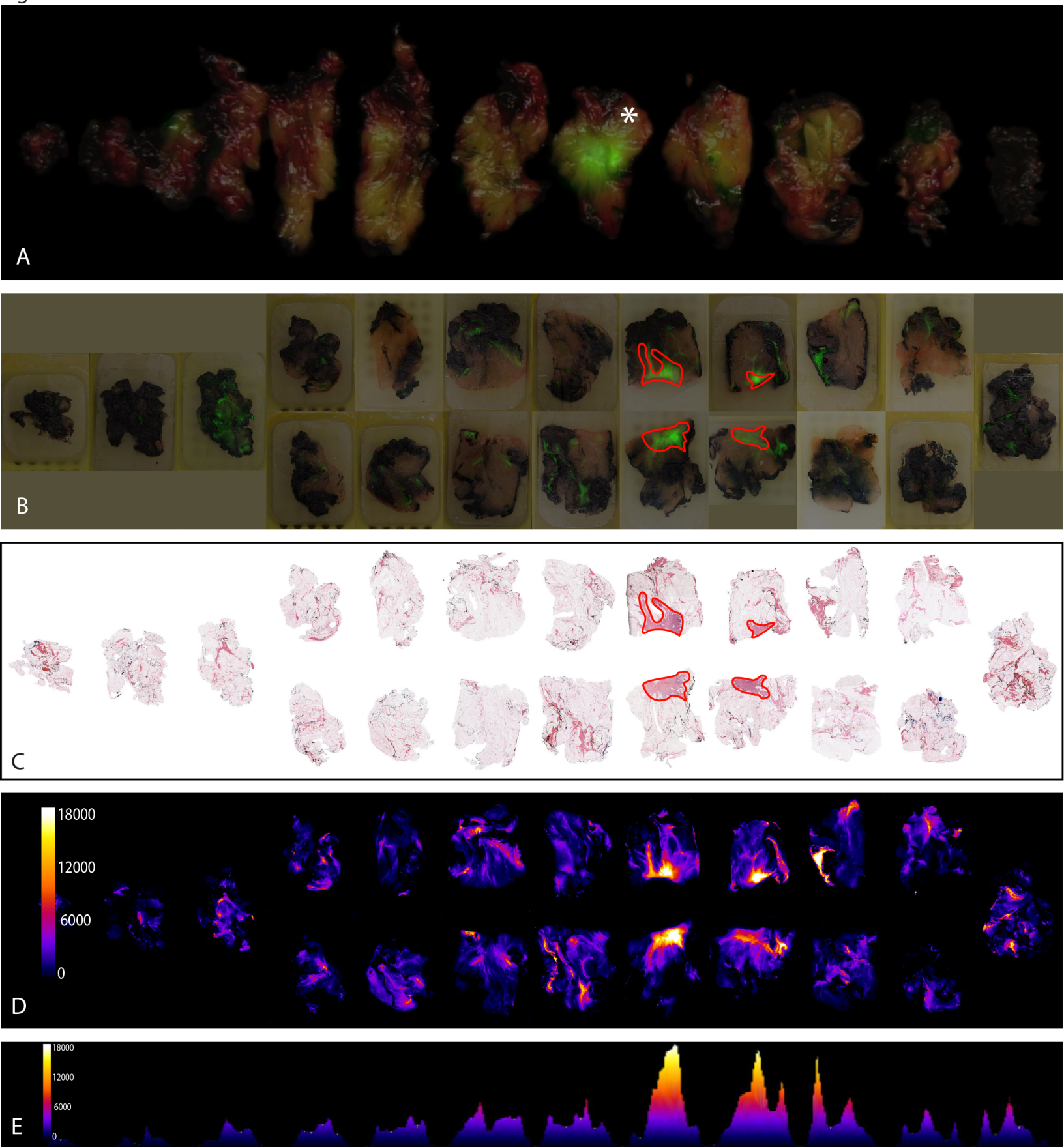


Figure 3

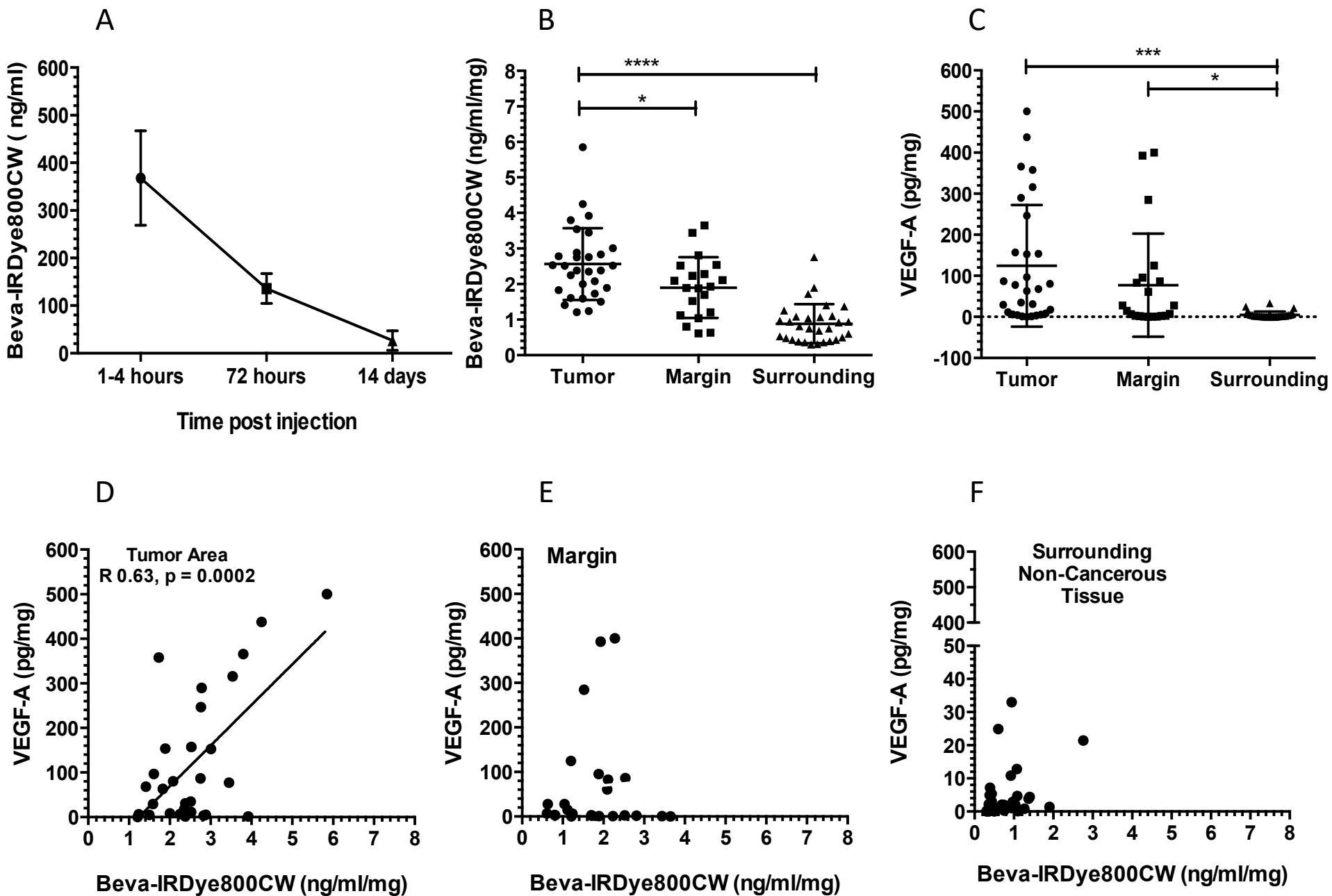


Figure 4

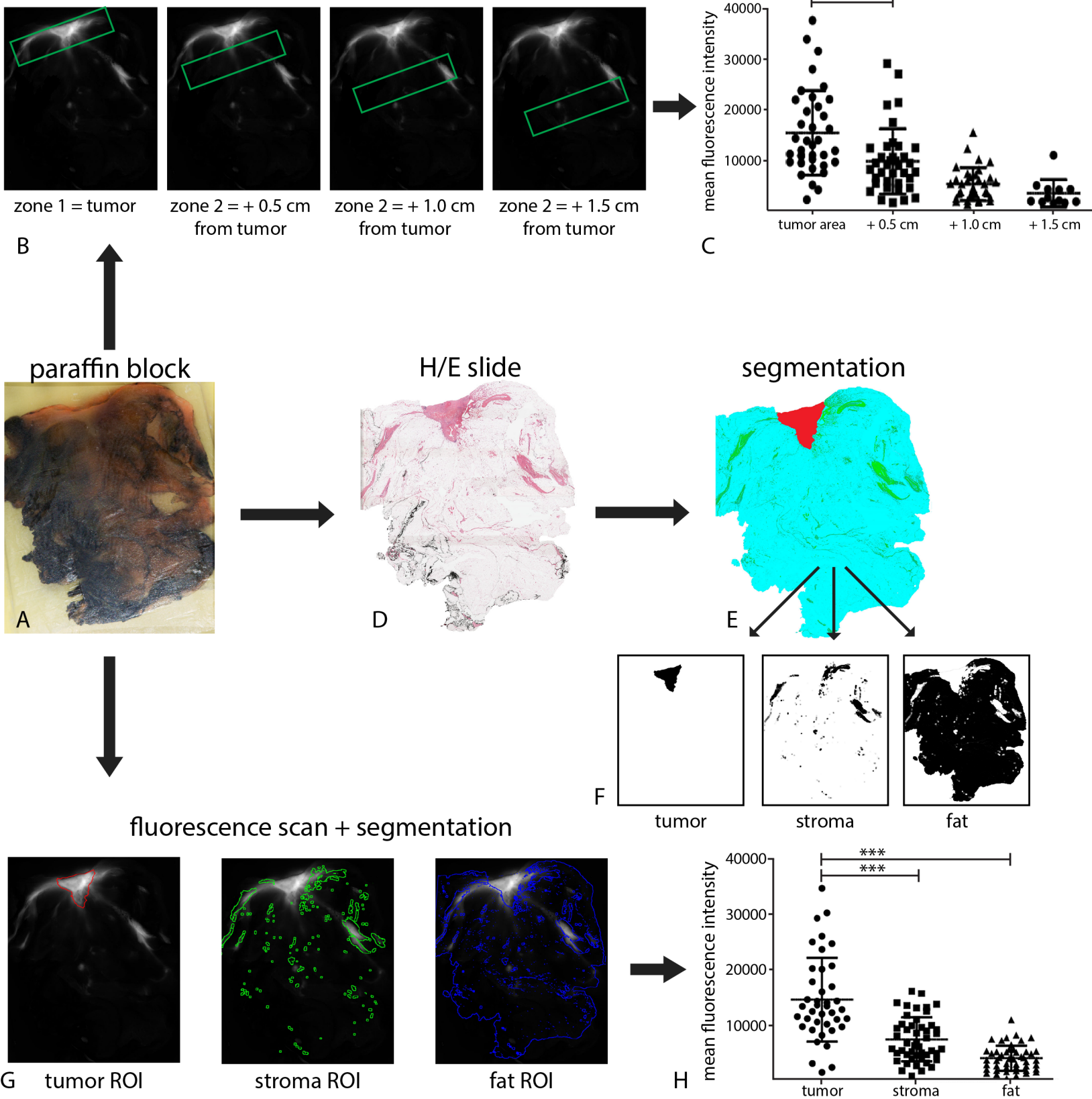
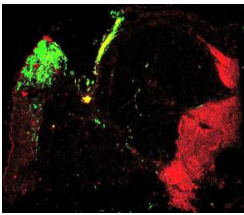
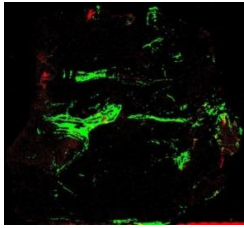
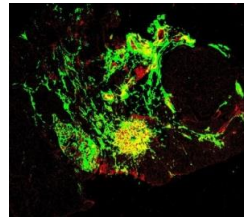
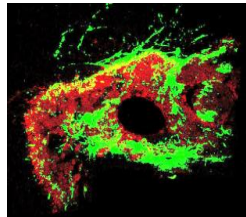
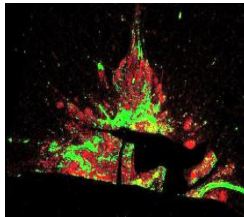
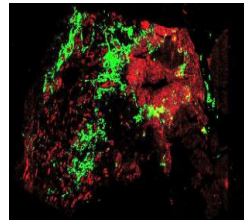
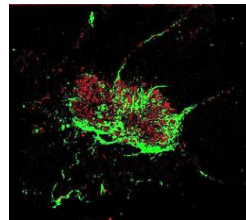
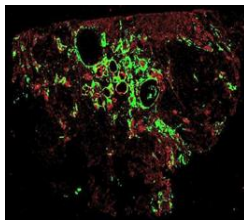
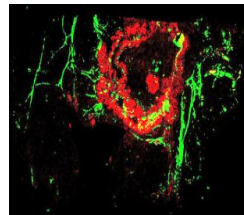
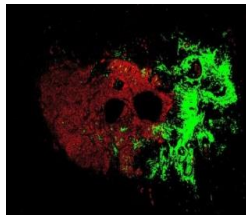
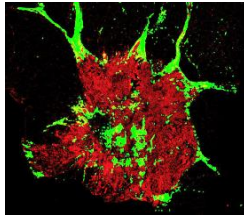
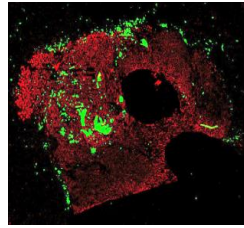
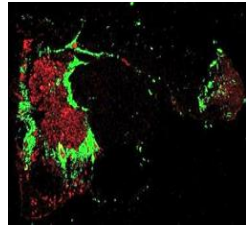
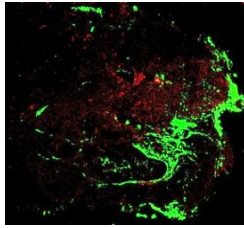


Figure 5

None (2/20)



Adjacent (12/20)



Overlap (6/20)

